Supplementary Information:

A shape-memory scaffold for macroscale assembly of functional nanoscale building blocks

Huai-Ling Gao‡, Yang Lu‡, Li-Bo Mao, Duo An, Liang Xu, Jun-Tong Gu, Fei Long, and Shu-Hong Yu*

I. Experimental

Preparation of highly porous chitosan scaffolds (CSSs).

Chitosan solution (2 wt %) was prepared by dissolving chitosan powder (1.0 g) in 50 mL of an aqueous solution of acetic acid (2 wt %). Chitosan scaffolds were fabricated according to the previously reported ice-templated process.[S1] Briefly, chitosan solution was poured into a silicon rubber mold placed at the top of a cold steel rod, which was cooled by liquid nitrogen, and frozen entirely. The shape of the scaffolds was adjusted by using different shapes of molds. The obtained frozen samples were then freeze-dried by using a Labconco-195 freeze-drier.

Synthesis of different nanoscale building blocks.

Highly water dispersible magnetite Fe_3O_4 NPs were synthesized by using a high-temperature hydrolysis reaction.[S2] Gold and silver nanoparticle colloid solutions were prepared by the Frens's method.[S3] Water soluble carbon nanotube (CNT) was prepared through the chemical oxidation treatment which was based on a mixture of concentrated nitric and sulphuric acids in a ratio of 1:3, respectively.[S4] Ag Nanowires were synthesized in a modified polyol reduction process reported by Yang et al.[S5] Te Nanowires were prepared according to a simple hydrothermal method developed by our group recently.[S6] Stable aqueous dispersions of reduced graphitic nanosheets (rGO) were prepared by reduction of the exfoliated GO (1 mg/mL)[S7] in the presence of PSS (10 mg/mL) under refluxing at 100 °C.[S8] Water-soluble CdTe QDs were synthesized according to previous reported literature.[S9] CdTe QDs with different emission spectra were acquired at four interval refluxing time.

Fabrication of multifunctional assemblies.

Ultimate assemblies (including CSS-Fe_3O_4NPs, CSS-AuNPs, CSS-AgNPs, CSS-CNT, CSS-AgNWs, CSS-TeNWs, CSS-rGO, and CSS-Fe_3O_4NPs-AgNWs) with different functionalities were prepared via constant adsorption of a certain concentration of different functional nanocrystals solution by CSSs (1.0 × 1.0 × 0.5 cm^3). The solutions of Fe_3O_4 NPs, CNT, Ag NWs, Te NWs and rGO-PSS were prepared by dispersing 1 mg nanocrystals into 6 ml water respectively.

The concentration of Au NPs and Ag NPs solution is 1.0 mM. The dried CSSs were first soaking into NaOH solution (1 wt %) for a while, and then washed with double distilled water to remove the NaOH. The next step involved direct electrostatic absorption of different nanocrystals into the CSSs. The purified CSSs were put into nanocrystals solution and squeezed repeated for several times by a tweezers, then color of the suspensions would faded away quickly and the assembled devices were yielded and freeze-dried.

Antibacterial performance test of the CSS-AgNPs.

In order to investigate the antibacterial Properties of the CSS-AgNPs, the wild-type E. coli inoculum was prepared by culturing a single colony from LB agar plates in 30 mL of LB fluid medium overnight at 37 °C in a shaker. Then the OD600 was measured to calculate the concentration of the bacterial suspensions by using a UV-Vis spectrophotometer. Sterilized solid culture medium plates were prepared previously. For zone of Inhibition test, 100 μL of E. coli (10^6 CFU/mL) was added to the plate and spread uniformly. Square shape of CSSs-AgNPs scaffold with two different amount Ag nanoparticles and Ag-free CSS (Length of side is about 5 mm) were gently placed onto the solidified agar gel in a same plate. The zone of inhibition was observed after incubation for 24 h at 37 °C. For another antibacterial test, the above two kinds of CSS-AgNPs and Ag-free CSS were first soaked into the E. coli medium which has been cultured overnight, and then were gently placed onto the solidified agar gel of a sterilized plate. The plate was then observed after incubation for 6 h at 37 °C.

Photothermal effect of CSS-AuNPs in aqueous solution.

CSSs absorbed with different amount of Au NPs was immersing in a 1.5 mL tube with 1.0 mL distilled water respectively. Then NIR with a wavelength of 808 nm and an output power of 2.0 w was irradiated to the CSS-AuNPs. The temperature change was measured every 1 min over a period of 10 min by using a digital thermometer (TES-1310, TES Electrical Corp.). Equal size of Au-free CSS was used as a control samples, and 1 ml water alone was used as blank control.

II. Characterization

Transmission electron microscopy (TEM) was performed on H-7650 (Hitachi, Japan) operated at an acceleration voltage of 100 kV. Scanning electron microscopy (SEM) was performed with a field emission scanning electron microanalyzer (Zeiss Supra 40) at an acceleration voltage of 5 kV. X-ray power diffraction (XRD) analyses were carried out on a Philips X'Pert PRO SUPER X-ray diffractometer equipped with graphite-monochromatized Cu Kα radiation. Zeta potential of different nanocrystals was measured by Nano Particle Analyzer (Delsa Nano C). Freeze drying was carried out using freeze-drier (Labconco-195). Laser device (MDL-808nm 2W) used in the photothermal test was made from Changchun New Industries Optoelectronics Tech.Co., Ltd. Water temperature was measured by digital thermometer (TES-1310, TES Electrical Corp.).

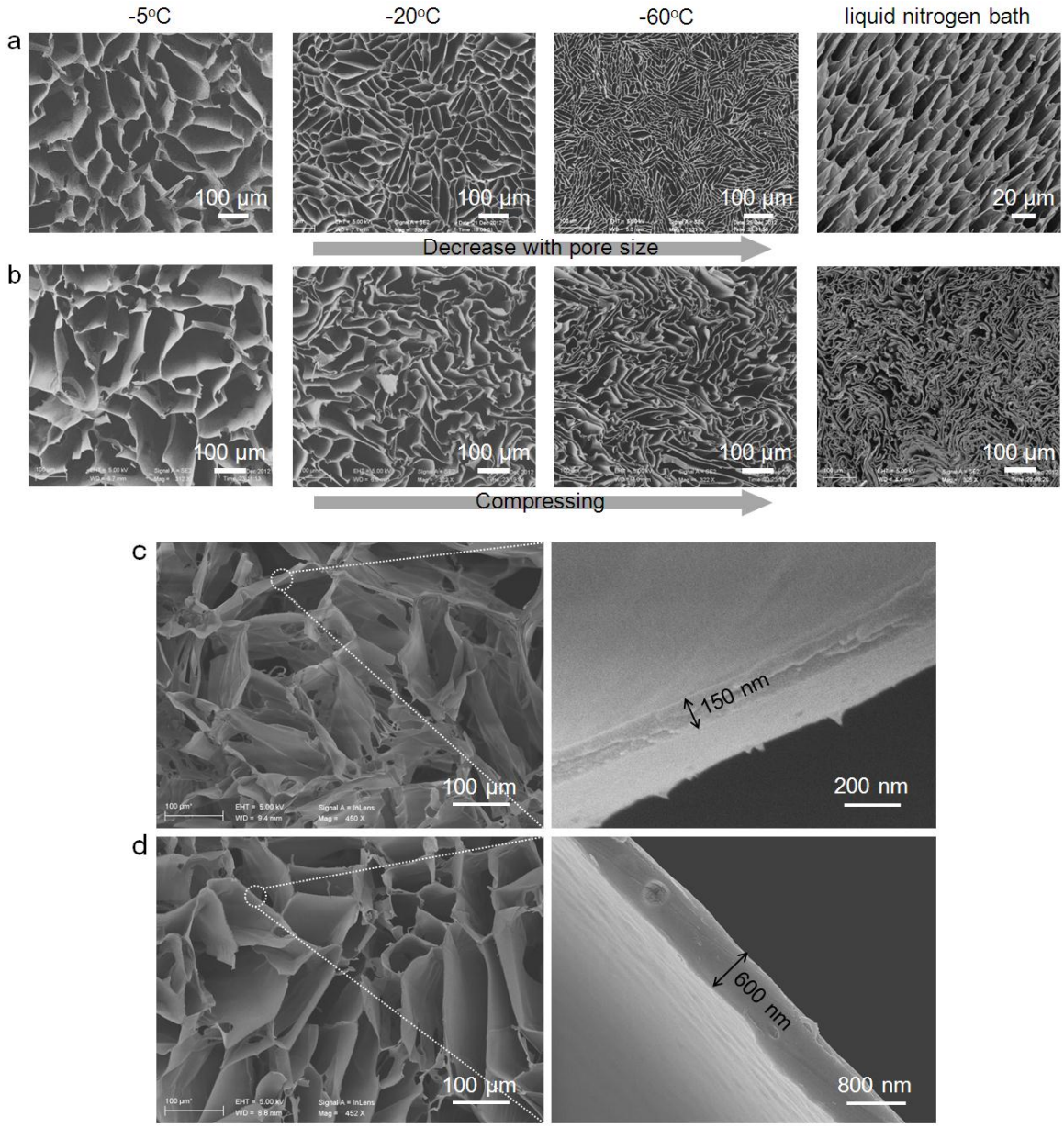

Fig. S1 SEM images show the cross section of CSSs with morphological characters. (a) CSS with decreasing pore channels (from 200 μm to 20 μm) was obtained by reducing the freeze temperature. (b) Large pore channels of CSS were compressed to smaller and smaller by using different compressing force. (c) The polymer walls of the scaffold which was made from 0.5 wt % chitosan solution are discrete and the average wall thickness is about 150 nm. (d) The polymer walls of the scaffold which was made from 2 wt % chitosan solution are continuous and the average wall thickness is about 600 nm.

Fig. S2 Photographs and SEM images show several kinds of water soluble polymer scaffolds. (a) Photographs of several kinds of water soluble polymer scaffolds fabricated through the same freeze casting process. (b) These several scaffolds made from only one polymer are easily be dissolved in water again and show no shape-memory property except to chitosan. (c) SEM images show that different polymer scaffolds have different morphologies of microstructure. Scale bars, 100 μm (c).

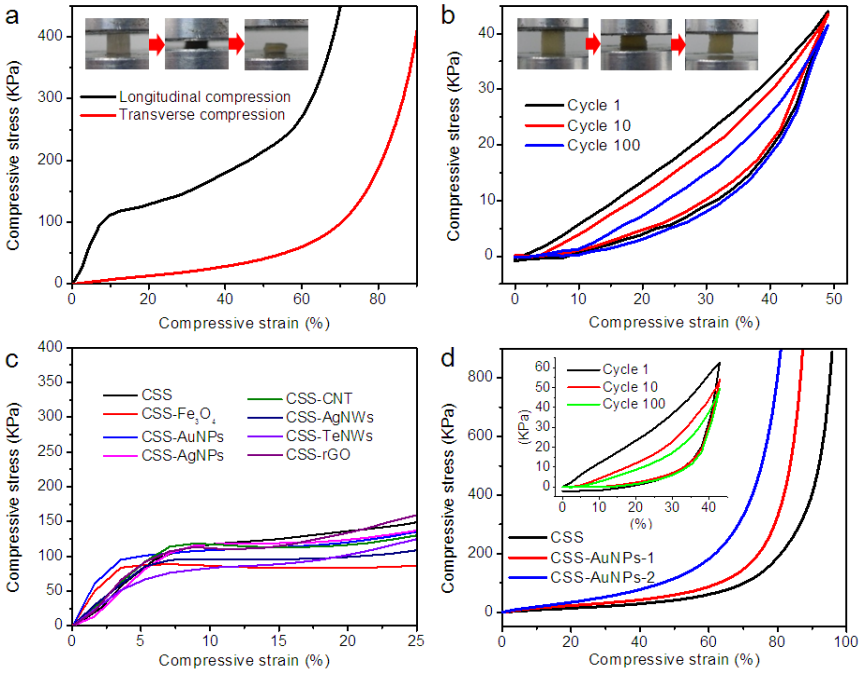

Fig. S3 Compressive stress–strain curves of the CSSs and nanocomposite CSSs. (a) CSSs were compressed along two different directions, which illustrate different mechanical properties parallel and perpendicular to the pore channel direction. The inset shows the permanent deformation of CSS when the compressive load was removed. (b) Cyclic stress–strain curves of CSS show the highly elastic compressibility perpendicular to the channel direction. The inset photograph shows only a small permanent deformation after 100 compression cycles at a maximum strain of 50%. (c) The compressive strength of CSSs in the longitudinal direction was almost unaffected after assembly into different nanocrystals. (d) The compressive strength of CSSs in the transverse direction was enhanced by assembly into AuNPs, while the elastic compressibility was weakened compared with pure CSSs. The insert shows the cyclic stress–strain curves of CSS-Au-1 which have assembled fewer AuNPs at a maximum strain of 40%.

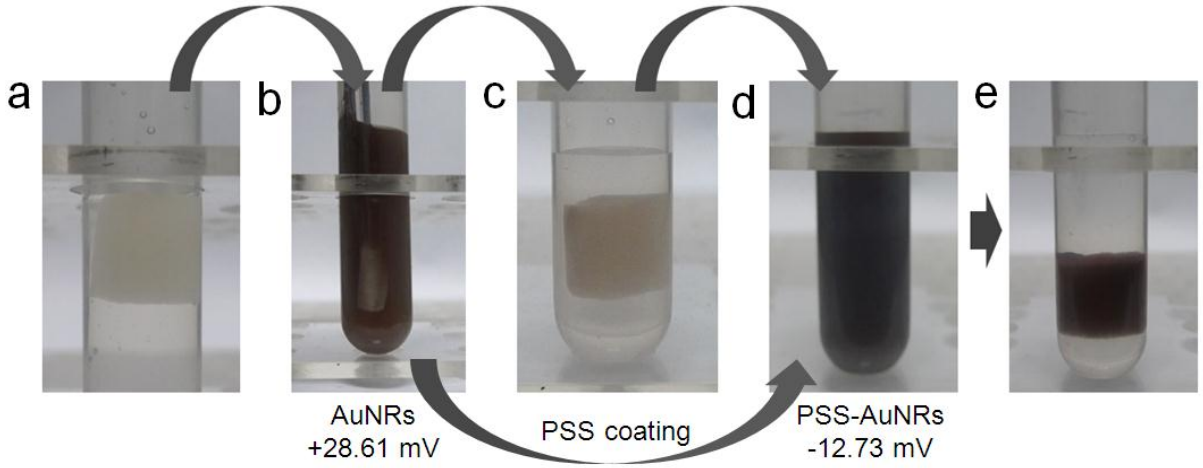

Fig. S4 Photographs of the adsorbing processes which show that only negative charged nanoparticles can be adsorbed effectively into chitosan scaffold.

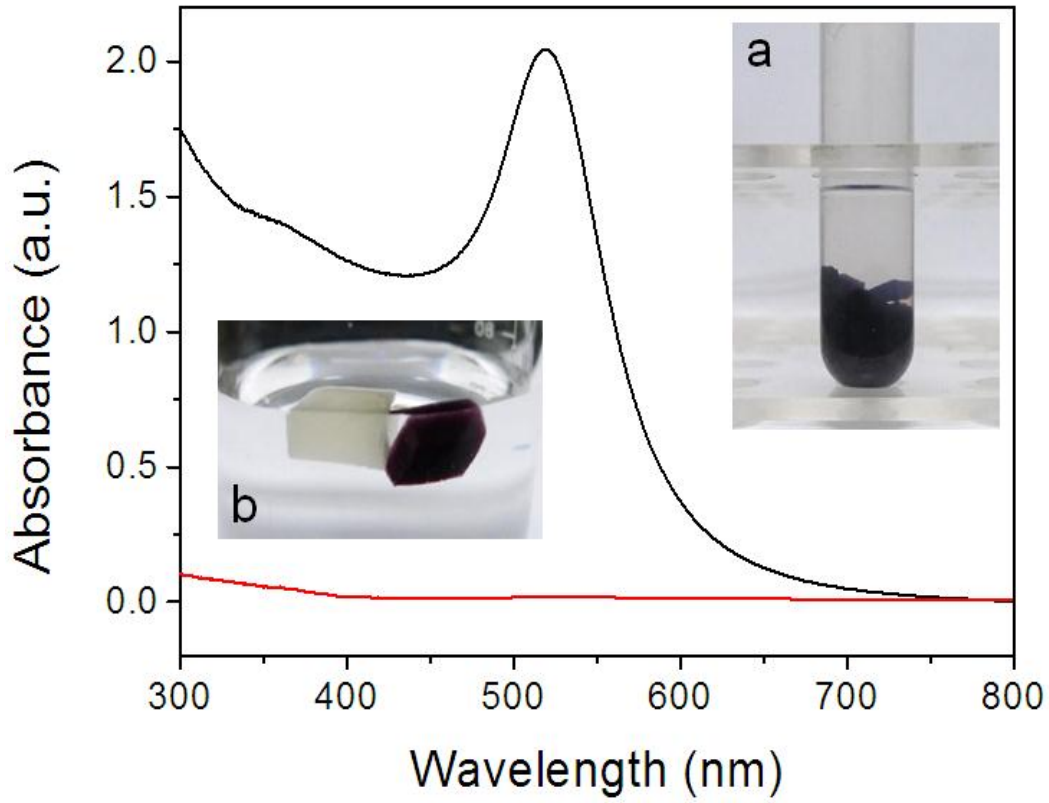

Fig. S5 UV-Vis spectra revealed that there is almost no release of AuNPs from CSS-AuNPs after two months soaking in water. Insert (a) is the corresponding photograph of CSS-AuNPs which have been cut into small pieces. The original size of CSS is 0.5 cm^3 and 10 ml AuNPs solution (1.0 mM) was adsorbed completely into it. Insert (b) shows that pure chitosan scaffold and CSS-AuNPs are the same stable after two months soaking in water.

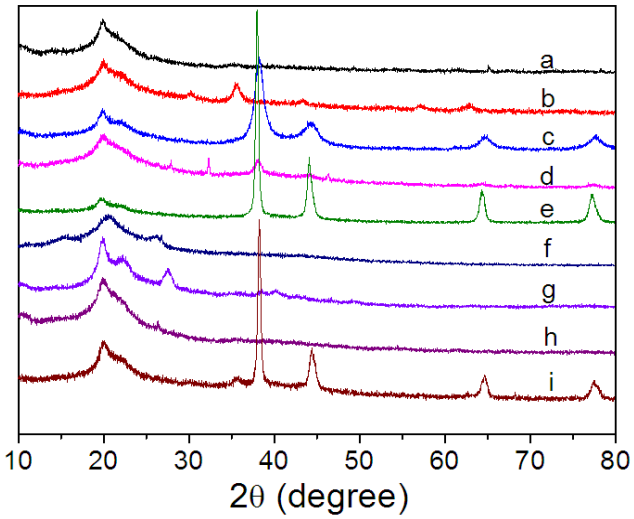

Fig. S6 XRD patterns of the compressed CSSs before and after integration of different nanocrystals. a-i are CSS, CSS-Fe_3O_4NPs, CSS-AuNPs, CSS-AgNPs, CSS-CNT, CSS-AgNWs, CSS-TeNWs, CSS-rGO, CSS-Fe_3O_4NPs-AgNWs, respectively.

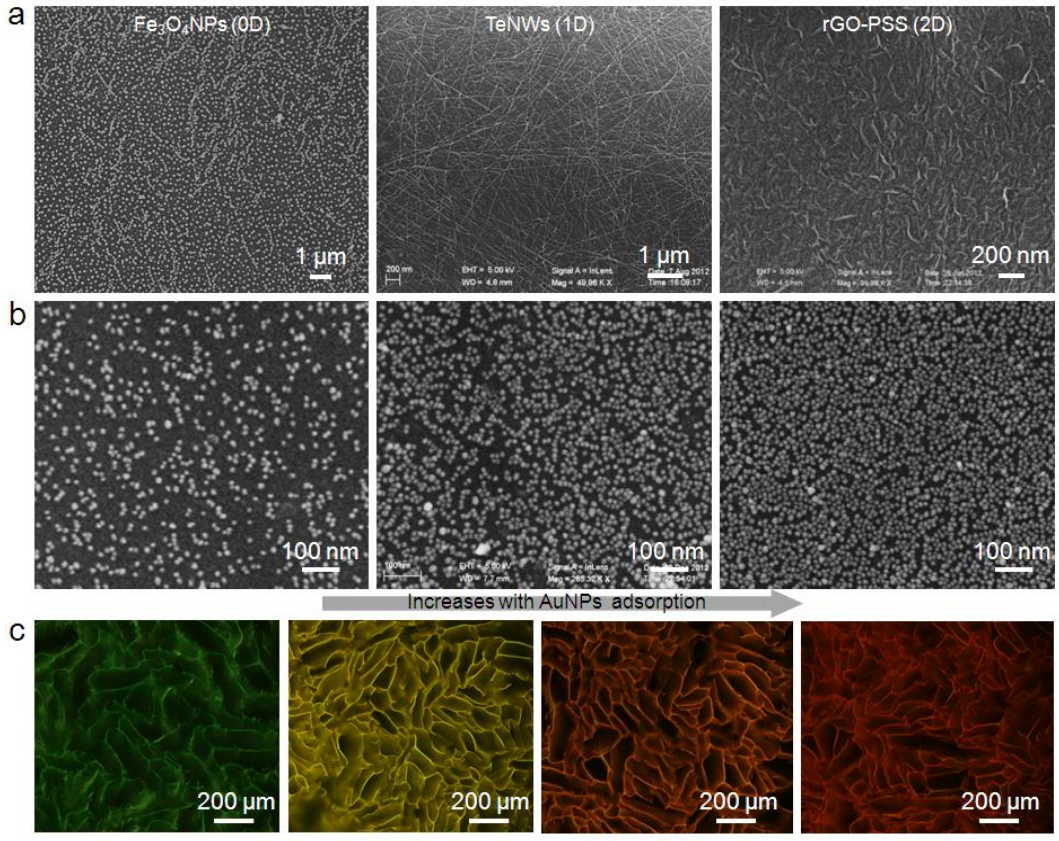

Fig. S7 SEM images and fluorescence microscope images showing the space distribution of nano-building blocks in CSSs. (a) Nanocrystals with different dimension located on the pore channel surface of CSSs. (b) Uniform distribution of AuNPs with growing density on the channel surface of CSSs. Here, 1.00 ml, 2.50 ml and 3.75 ml AuNPs solution (1.0 mM) was absorbed completely by a piece of CSS with the volume of 0.25 cm^3 from left to right. (c) Cross section of CSSs which have been integrated with different emission spectrum of CdTe QDs. The corresponding fluorescent assemblies are shown in Figure 3d.

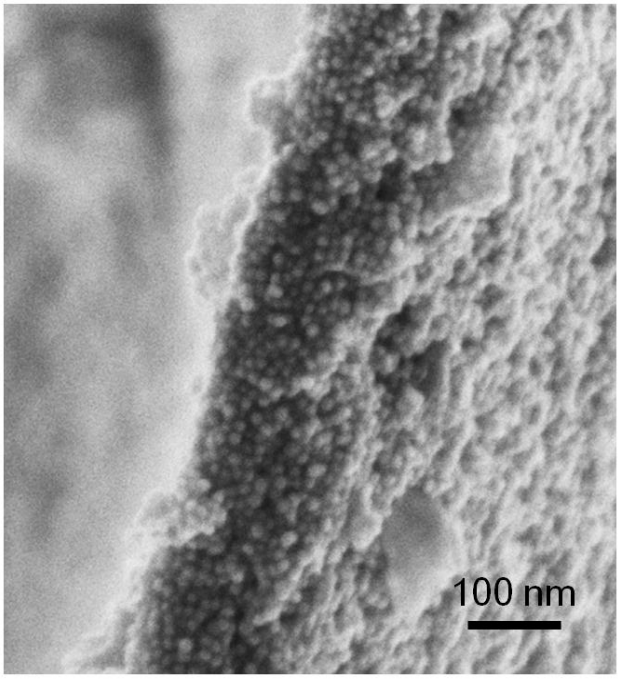

Fig. S8 SEM images showing the compactly distribution of AuNPs on the polymer wall of the channel surface of CSS.

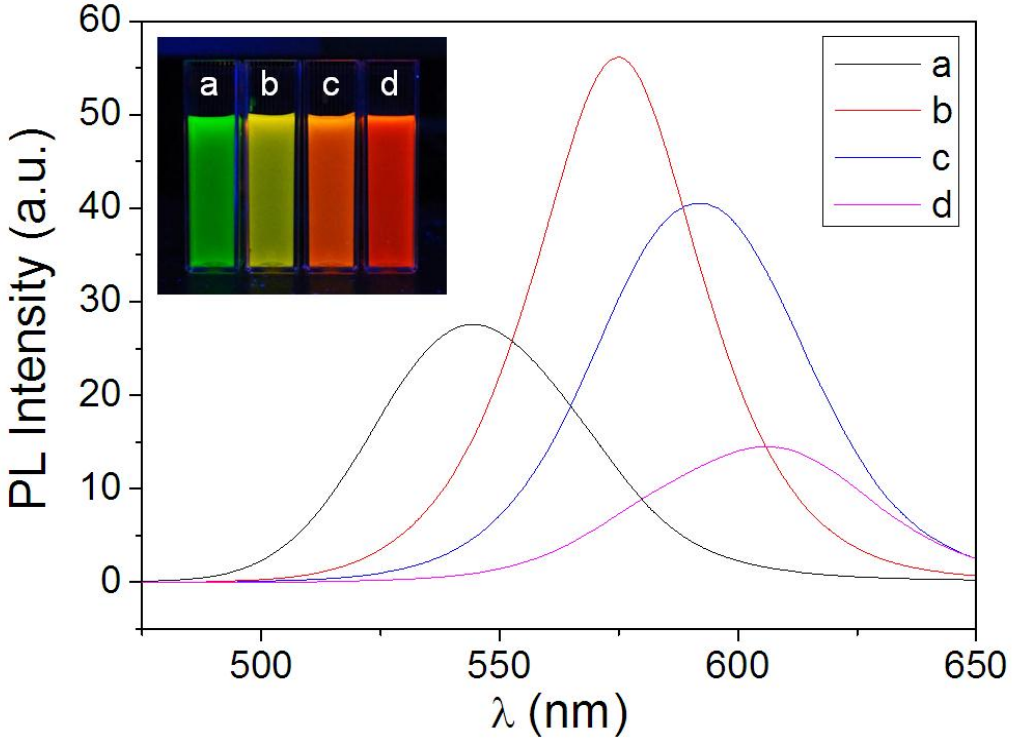

Fig. S9 Emission spectra of the CdTe QDs acquired at four interval reaction time. The inset (a) displays the corresponding emission color of the CdTe QDs aqueous solution. The inset (b) demonstrates the fluorescent CSSs which were composited with the corresponding CdTe QDs.

Table S1. Characteristics of CSSs with ultra-high porosities of >97% and ultra-strong water absorption. CSSs with weight of 0.03 g can hold 0.67 g water and approximately 0.60g water can then be released from the sample by compression.

Porosity	97.48%± 0.16%
Water absorption	2231.41%±79.46%

Table S2. Zeta potential of the several types of nanocrystals which were absorbed by the CSSs under the condition at pH 7.

Sample	**Zeta potential (mV)**
Fe_3O_4NPs	-30.16±7.94
AuNPs	-46.06±6.27
AgNPs	-58.93±7.79
CNT	-28.1±1.74
AgNWs	-12.19±2.65
TeNWs	-27.73±3.12
rGO-PSS	-64.59±4.95
CdTe QDs	-35.56±2.43

References

S1 S. Deville, E. Saiz, R. K. Nalla, A. P. Tomsia, *Science* 2006, **311**, 515.

S2 J. P. Ge, Y. X. Hu, M. Biasini, W. P. Beyermann, Y. D. Yin, *Angew. Chem. Int. Ed*. 2007, **46**, 4342.

S3 G. Frens, *Nature-Physical Science* 1973, **241**, 20.

S4 M. S. P. Shaffer, X. Fan, A. H. Windle, *Carbon* 1998, **36**, 1603.

S5 C. Yang, H. W. Gu, W. Lin, M. M. Yuen, C. P. Wong, M. Y. Xiong, B. Gao, *Adv. Mater.* 2011, **23**, 3052.

S6 H. S. Qian, S. H. Yu, J. Y. Gong, L. B. Luo, L. F. Fei, *Langmuir* 2006, **22**, 3830.

S7 W. S. Hummers, R. E. Offeman, *J. Am. Chem. Soc.* 1958, **80**, 1339.

S8 S. Stankovich, R. D. Piner, X. Q. Chen, N. Q. Wu, S. T. Nguyen, R. S. Ruoff, *J. Mater. Chem.* 2006, **16**, 155.

S9 H. Zhang, Z. Zhou, B. Yang, M. Y. Gao, *J. Phys. Chem. B.* 2003, **107**, 8.